Impact of a staggered scaffold structure on the mechanical properties and cell response in bone tissue engineering

Xiaoli He[1,2,3] iD **, Qian Zhao[1,2], Ningning Zhang[1,2], Junbin Wang[1,2], Qingzong Si[1,2], Ying Xue[4] and Zhe Xing[1,2,5]** iD

Abstract

The primary goal of bone tissue engineering is to fabricate scaffolds that can provide a microenvironment similar to that of natural bone. Therefore, various scaffolds have been designed to replicate the bone structure. Although most tissues exhibit complicated structures, their basic structural unit includes stiff platelets arranged in a staggered micro-array. Therefore, many researchers have designed scaffolds with staggered patterns. However, relatively few studies have comprehensively analyzed this type of scaffold. In this review, we have analyzed scientific research pertaining to staggered scaffold designs and summarized their effects on the physical and biological properties of scaffolds. Compression tests or finite element analysis are typically used to evaluate the mechanical properties of scaffolds, and most studies have performed experiments in cell cultures. Staggered scaffolds improve mechanical strength and are beneficial for cell attachment, proliferation, and differentiation in comparison with conventional designs. However, very few have been studied in vivo experiments. Additionally, studies on the effect of staggered structures on angiogenesis or bone regeneration in vivo, particularly in large animals, are required. Currently, with the prevalence of artificial intelligence (AI)-based technologies, highly optimized models can be developed, resulting in better discoveries. In the future, AI can be used to deepen our understanding on the staggered structure, promoting its use in clinical applications.

Keywords

Staggered structure, scaffold, bone tissue engineering, cell response

Introduction

Recently, the segmental repairing of bone defects has garnered significant attention for orthopedic and plastic surgeries. Currently, autologous and allogeneic transplantations are used in clinical practice for bone repair and regeneration.[1] Autografts are regarded as the "gold standard," achieving varying degrees of success in restoring bone function, owing to their high histocompatibility and low immunogenicity.[2] However, harvesting autogenous bone from the iliac crest or other sites may come with surgical risks such as scarring, bleeding, inflammation, and chronic pain.[3,4] These limitations hamper their extensive use in clinical applications.

To address this challenge, scaffold-based tissue engineering provides a new approach toward repairing bone defects. Scaffolds are significant as they can provide an

[1]School/Hospital of Stomatology, Lanzhou University, Lanzhou, Gansu Province, China
[2]Key Laboratory of Dental Maxillofacial Reconstruction and Biological Intelligence Manufacturing, Lanzhou University, Lanzhou, Gansu Province, China
[3]The Affiliated Stomatological Hospital of Southwest Medical University, Luzhou, Sichuan Province, China
[4]Department of Clinical Dentistry, Faculty of Medicine, University of Bergen, Bergen, Norway
[5]Department of Medical Biology, Faculty of Health Sciences, UiT The Arctic University of Norway, Tromsø, Norway

Corresponding authors:
Zhe Xing, RNA and molecular pathology research group (RAMP), Department of Medical Biology, Faculty of Health Sciences, UiT The Arctic University of Norway, Tromsø 9037, Norway.
Email: zhe.xing@uit.no

Qingzong Si, School/Hospital of Stomatology, Lanzhou University, Donggang West Road 199, Lanzhou, Gansu Province 73000, China.
Email: siqz@lzu.edu.cn
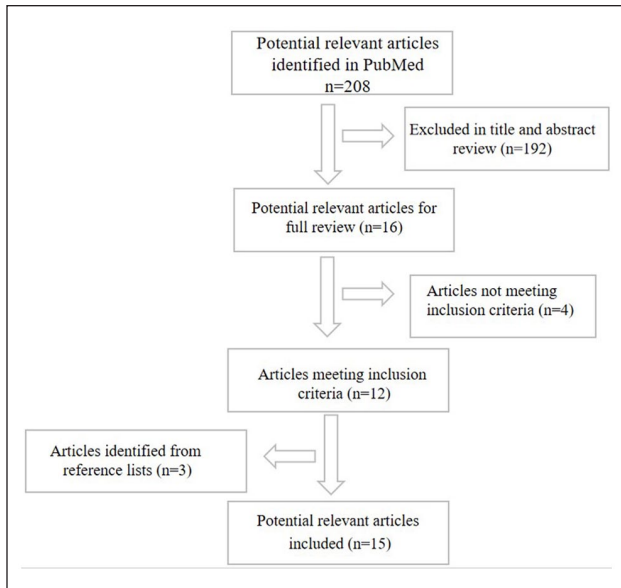
Figure 1. The flow chart of literature selection for the review.

ideal environment for cell growth and differentiation, contributing to the development of new bone tissue.[5] Apart from scaffold porosity and pore size,[6] new tissue formation is significantly influenced by the 3D structure of the scaffold.[7] Scaffold architecture can also influence nutrient transport and cell–matrix interaction. Therefore, based on the natural bone hierarchical structure, researchers have designed various scaffold architectures at the macroscale, microscale, and nanoscale.[5] Additionally, recent studies have demonstrated new design patterns for staggered structures. However, relatively few studies have comprehensively analyzed this type of scaffold. The functionality of scaffolds is determined by their permeability, and mechanical and biological properties.[8] Therefore, the aim of this review is to summarize current scientific research regarding the effects of the staggered structure on the physical as well as biological properties of scaffolds.

Literature survey

In this review, systematic literature search was carried out on "PubMed." The keywords used to collect relevant literature were "staggered, tissue engineering, scaffold," "shift, tissue regeneration, scaffold," "offset, tissue engineering, scaffold," and "compacted, tissue engineering, scaffold." Only original research studies evaluating the impact of the staggered, shift, offset, or compacted designs on the physical and chemical properties or cell response were selected (Figure 1). Review articles, studies with insufficient data, and research articles that did not aim to regenerate the bone for clinical applications were excluded. The scaffold materials, fabrication methods, experiment content, and design details of the related studies are summarized in Table 1. A narrative review regarding the

detailed methodology, physical properties, cell response, and bone regeneration is also provided.

Staggered structures in porous scaffolds

Evaluation methods

Only 15 studies sufficiently met the inclusion criteria. A compression test and finite element analysis (FEA) are two methods typically used to evaluate the mechanical properties of printed scaffolds. Further, FEA predictions and the actual compression moduli of the fabricated scaffolds exhibited similar trends. Cho et al.[11] designed and fabricated scaffolds with lay-down, offset, and dual-pore kagome-structure design, named Conv 1, Conv 2, Offset 1, Offset 2, and dual-pore scaffolds, and evaluated their compression moduli via numerical and experimental analyses. Compared with the results of numerical analysis, experimental analysis yielded compression moduli showed the similar results (numerical and experimental analyses yielded compression moduli of 65 and 62.5 ± 1.8 MPa, respectively, for Conv 1). Additionally, most studies performed in vitro experimental studies to evaluate their biological properties, whereas only two studies performed in vivo experiments.

Fabrication methods

In these designs, two typical scaffold fabrication methods are three-dimensional (3D) printing and melt electrowriting (MEW), although there are many methods that could be used for scaffold fabrication.3D printing, an additive manufacturing (AM) process, prepares scaffolds via a layer-by-layer process and has been widely used to design and fabricate porous scaffolds.[25,26] It consists of five main components, as shown in Figure 2(a).[7] It is advantageous as it can fabricate scaffolds that imitate the extracellular matrix (ECM). In addition, it can control porosity, pore size, and pore distribution,[24] and produce complex 3D structures. However, the scale of the fibers that form the scaffolds ranges from hundreds of microns to millimeters,[25] which is considerably larger than the scale of the ECM or cells (10–20 μm). Therefore, it cannot create a favorable microenvironment for cells. Two studies fabricated scaffolds using MEW, a high-resolution AM technology capable of producing small fibers from 800 nm to 50 μm in diameter.[26,27] MEW[25] consists of four components: collector, high voltage source, pneumatic system, and electrically-heated system (Figure 2(b)) .[19] In particular, when the collector speeds of MEW are not synchronized with the electrified jet speed, buckling jetting is likely to occur,[28] thereby producing an array of different modeled and predicted patterns.[29] Hochleitner et al.[30] fabricated fibrous scaffolds with sinusoidal patterns using MEW.

Table 1. Overview of the eligible studies.

Scaffold Material	Fabrication Method	Experiment content	Design details	Reference
Polycaprolactone (PCL) and hydroxyapatite (HA)	3D Printing	Mechanical properties cell attachment in vitro	PCL, PCL/HA, PCL/HA/SP	Park et al.[9]
HA and demineralized bone matrix (DBM)	3D Printing	Bone regeneration vascularization in vivo	90°/500 mm/aligned, 45°/500 mm/aligned, 90°/1000 mm/aligned, 45°/1000 mm/aligned, 90°/1000 mm/offset, 45°/1000 mm/offset	Hallman et al.[10]
Nano-hydroxyapatite (nHA) and PCL	3D-Printing	Compressive modulus (FEA) Cell adhesion, proliferation, and ALP concentration in vitro	Lay-down, offset, and dual-pore patterns	Cho et al.[11]
Gelatin, HA	3D printing	Cell proliferation and osteogenic differentiation in vitro	Double-layer orthogonal (GEHA20) double-layer staggered orthogonal (GEHA20-ZZ orGEHA20-ZZS double-layer alternative structure (GEHA20-45or GEHA20-45S)	Kim et al.[12]
PCL	3D printing	Mechanical properties cell adhesion, proliferation, and ALP concentration in vitro	Basic, basic-offset, crossed, and crossed-offset	Yilgor et al.[13]
PCL	3D printing	The mode of growth factor delivery Cell proliferation in vitro	The oriented scaffolds (basic, basic-offset) random scaffolds	Yilgor et al.[14]
PCL	3D printing	Compressive modulus Cell response in vitro	Scaffolds with 45° and 90° layer rotation	Sun et al.[15]
PCL/alginate	3D printing	Compressive modulus Cell response in vitro	A multi-layered 3D structure with a 100% offset for each layer	Kim et al.[16]
PCL	3D printing	Compressive modulus Cell response in vitro	0/90°, 0/90° S, 0/45°, and 0/90° NP	Declercq et al.[17]
SPCL	3D printing	Compressive modulus Cell response in vitro	Homogeneous scaffolds with pore sizes of 0.75 and 0.1 mm	Sobral et al.[18]
calcium phosphate (CaP) and PCL	MEW	In vivo and FEA	Scaffolds with pore sizes of 250 and 500 μm, Scaffolds with pore sizes of 500 μm with 50% fiber offset Scaffolds with different pore sizes: 750–500–250 μm (grad.750top) and 250–500–750 μm (grad.250top)	Abbasi et al.[19]
PCL and poly (lactide-co-glycolide)	3D printing	Compressive modulus Cell response in vitro	Scaffolds with lattice, stagger, and triangle design	Lee et al.[20]
PCL	3D printing	Compressive modulus and FEA	Gradient (G) gradient and staggered (GS)	Liu et al.[21]
Polycaprolactone PCL-beta-tricalcium phosphate (PCL–β-TCP)	3D printing	Compressive modulus Cell response in vitro	Scaffolds with the offset value (0%, 25%, 50%, 75%, and 100%)	Yeo et al.[22]
PCL	MEW	Cell response in vitro	Scaffolds with different pore sizes of 250, 500, or 750 μm Scaffolds with 30% or 50% offset gradient scaffold with pore sizes of 250–500 - 750 μm	Abbasi et al.[23]

Staggered scaffold structures

Different staggered scaffold structures. The varied structuring over multiple lengths and material properties of hard biological tissues are significant in biomechanical research.[31] Most of these tissues have complex shapes, but their basic building units typically consist of stiff platelets arranged in a staggered micro-array inside a flexible matrix.[32] These basic building blocks are characterized by a periodic unit. As shown in Figure 3,[31] they consist of two regions: overlap and gap. The former comprises of two overlapping platelets while the latter is the space between two platelet ends.

Based on the geometric properties of the tissue, the researchers have arranged scaffolds in a staggered micro-array. Five types of arrays, designed based on differences between the overlapped sections, are shown in Figure 4.[22] The first layer is printed, and the second layer is printed with different offset values (0%–100%) relative to the first layer. The third and fourth layers are plotted with geometries identical to the first and second layers, respectively.[22]

Effect of the staggered structure on physical properties. In scaffolds used for bone tissue regeneration, appropriate mechanical properties that resist physiological loading and are similar to those of bone tissue, are highly desirable.[33,34] Therefore, designing various scaffolds to achieve satisfactory mechanical properties is crucial. Recently, some studies have focused on characterizing the mechanical properties of the staggered structure (Table 2).[9–13]

First, researchers discovered that the compressive strength or modulus of materials can be varied when the scaffold arrays are staggered. Yilgor et al.[13] designed four different poly(ε-caprolactone) (PCL) scaffolds as follows: basic (B), basic-offset (BO), crossed (C), and crossed-offset (CO). All the scaffolds were fabricated via the consecutive deposition of the 2D layers. The B architecture of the second layer is plotted orthogonal to the first layer. While the BO architecture showed a similar structure to B, the second layer is printed with an offset relative to the first layer. The first layer of the C architecture is plotted diagonal to the second layer. Further, the second layer of the CO architecture is printed offset relative to the first layer. The compression moduli of the BO and CO scaffolds are different from that of the B and C scaffolds, respectively. Sobral et al. designed four types of scaffolds, including those with fiber distances of 0.75 (Homog 1) and 0.1 mm (Homog 2), and two scaffolds whose pore size varied with depth, which were named Grad 1 and Grad 2. They observed that the Young's modulus of the scaffolds with an offset (Grad 1 and Grad 2) are in between Homog 1 and Homog 2. This phenomenon might be attributed to the different porosities of those scaffolds. However, the stress-strain curve plotted for all the samples showed a non-linear correlation, indicating that compression strength modulation was also affected by the orientation and relative location of the fibers along the scaffold.[18,35,36] Park et al.[9] used PCL and hydroxyapatite (HA) to design three types of scaffolds, including PCL (fabricated without a shifted pattern), PCL/HA (fabricated without a shifted pattern using PCL and HA), and PCL/HA/SP scaffolds (fabricated in a shifted pattern) using a bio-plotting system. They had similar porosities as follows: PCL (91.15), PCL/HA (92.01), and PCL/HA/SP (92.55). Further, compared with the PCL/HA/SP scaffold, compressive testing showed that the compression moduli of the no-shift scaffold (PCL and PCL/HA) were significantly higher. This is due to the juxtaposition of consecutive filaments of the PCL and PCL/HA scaffolds along the z-axis. Similarly, Cho et al.[11] designed PCL/nHA layer-down (Conv 1 and Conv 2), offset (Offset 1 and Offset 2), and a dual-pore Kagome scaffolds. With the same pore size and porosity, the compression moduli of scaffolds with the layer-down patterns were higher compared to those of scaffolds with offset patterns. Sun et al.[15] designed 0/45 (45° layer rotation) and 0/90 scaffolds (90° layer rotation with layer offset of 0.7 mm) with similar porosities and identical sizes. The compression test showed that the 0/90 scaffold was softer than the 0/45 scaffold. Liu et al.[21] demonstrated that the scaffold stiffness was 1.07 MPa under compression and 0.97 MPa under tension when the scaffold was designed with a gradient and staggered geometry.

Furthermore, for different offset scaffold patterns, their stress and strain curves demonstrate different trends. Cho et al.[11] prepared PCL/nHA scaffolds with offset patterns (Offset 1 and Offset 2) and experimentally evaluated their compression moduli to be 41.3 ± 3.9 and 12.0 ± 1.1 MPa, respectively. A similar finding was also reported in another similar study.[22] Yeo et al.[22] designed scaffolds with 0%, 25%, 50%, 75%, and 100% offset values using Polycaprolactone-beta-tricalcium phosphate (PCL-β-TCP) and calculated their elastic moduli (E) for bending. For similar porosity, the elastic modulus of PT-100 (scaffolds with 100% offset values) was 7.4% higher than that of PT-0 (scaffolds with 0% offset values).

More importantly, researchers observed that the compressive strength of scaffolds were 4–12 MPa and the compressive moduli were 67–445 MPa, comparable to the human trabecular bone.[37] Lee et al.[20] designed scaffolds with identical porosity, strand width, and space, but different structures (lattice, staggered, and triangular) using PCL and poly (lactide-co-glycolide) with compression strengths of 6.05, 7.43, and 9.81 MPa, respectively. and compression moduli of 120.2, 122.3, and 178 MPa, respectively.

In addition to its mechanical properties, the staggered structure can also influence the water-uptake ability and flow velocity of the scaffold. Surface hydrophilicity plays an important role in cell attachment. Dowling et al.[38] reported that the optimum water contact angle for cell adhesion was approximately 64°. Yeo et al.[22] reported that
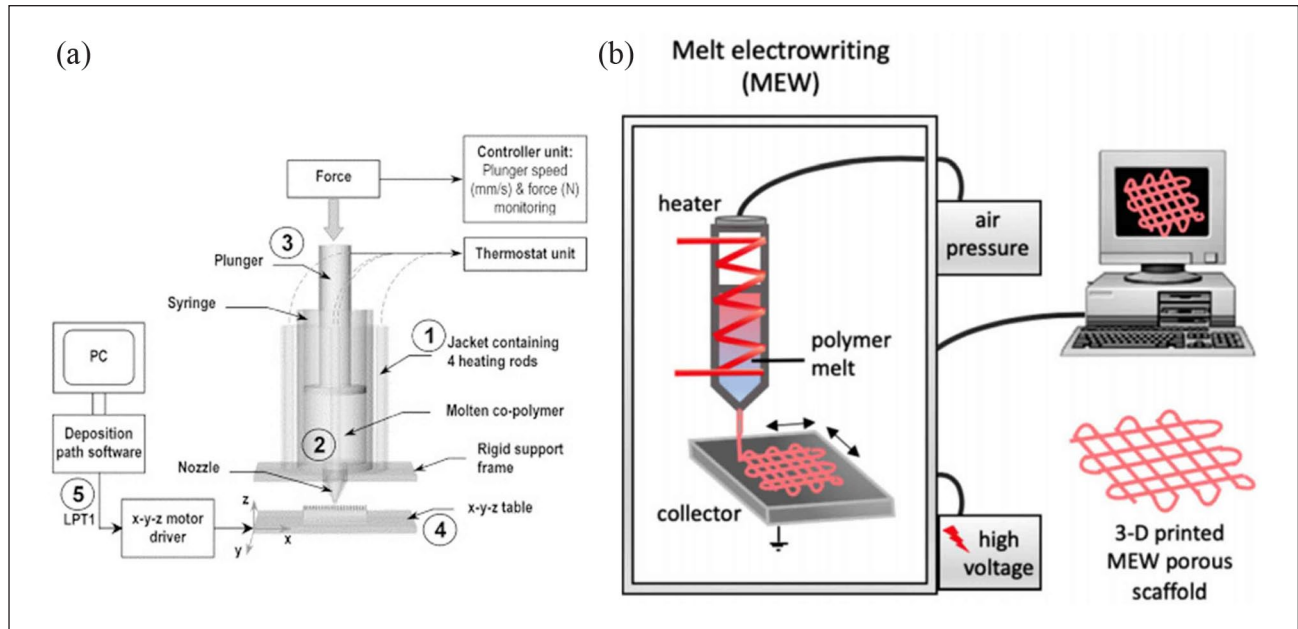
Figure 2. Primary components of 3D deposition and MEW. (a) 3D printing device consisting of five main parts: (1) jacket, (2) molten unit, (3) force-controlled plunger, (4) XYZ table, and (5) X-Y-Z motor driver.[7] Copyright © 2003 Elsevier Ltd. (figure reused with permission). (b) MEW consisting of four parts: collector, high voltage source, pneumatic system, and electrically-heated system.[19] Copyright ©2020 by the Naghmeh Abbasi (figure reused with permission).
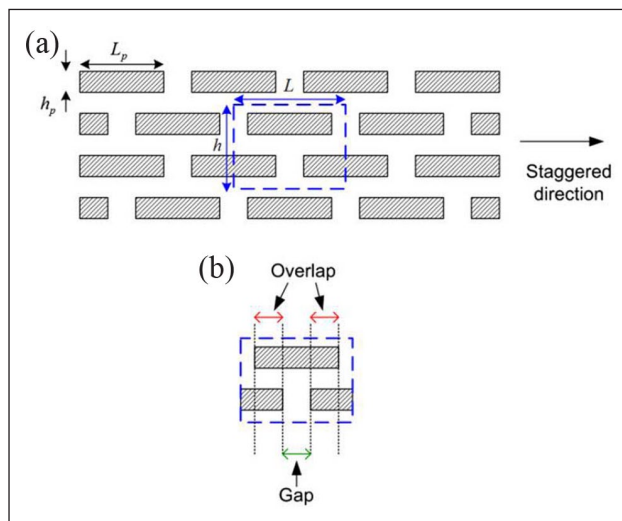

Figure 3. (a) Schematic of a staggered scaffold (L represents length, H represents height) (b) The two regions in a staggered microstructure: Overlap and Gap regions. The former consists of two overlapping platelets and the latter is the space between two platelet ends.[31] Copyright ©2011 Elsevier Ltd. (figure reused with permission).

the water uptake of the offset scaffolds was higher compared with that of no-offset scaffolds (PT-0). Moreover, PT-0 had the highest flow speed, and flow velocity gradually decreased with increasing offset value.

Effect of the staggered structure on biological properties. Scaffolds with staggered structures fabricated via 3D printing, which affect the cellular response during tissue regeneration, have been extensively studied in vitro (Table 2).[9,11–13,17,18,22] Firstly, the offset patterns in the staggered structures cause a spatial-pore-size gradient to some extent. Therefore, the cell seeding efficiency and distribution are improved. Declercq et al.[17] prepared scaffolds with 0/90, 0/45, 0/90 S (0/90 with shifted patterns), and 0/90 NP (0/90 with pore size of 200 µm). Mouse calvaria pre-osteoblast cells (MC3T3-E1) were seeded into the scaffolds, and the seeding efficiency was tested after 1 day. For the conventional 0/90 design, the cell seeding efficiency was $52.2 \pm 2.3\%$, and those of the 0/90 S, 0/45, and 0/90 NP were $66.4 \pm 3.4\%$, $69.5 \pm 3.7\%$, and $78.02 \pm 5.1\%$, respectively. Thus, an obstructed architecture improved seeding efficiency. Yeo et al.[22] reported that scaffolds with offset patterns (particularly ones with 100% and 50% offset values) exhibited higher efficiencies than no-offset scaffolds as the scaffolds with offset patterns had suitable pore size and slightly complex microstructure. Moreover, 3D printed scaffolds with different offset allow homogenous cell growth. Sobral et al.[18] reported that a more even distribution of cells in Grad 1 scaffolds compared to Grad 2 scaffolds.

Secondly, staggered patterns influence cell proliferation. Yilgor et al.[13] seeded a rat bone marrow mesenchymal stem cell on PCL scaffolds. They reported the cell
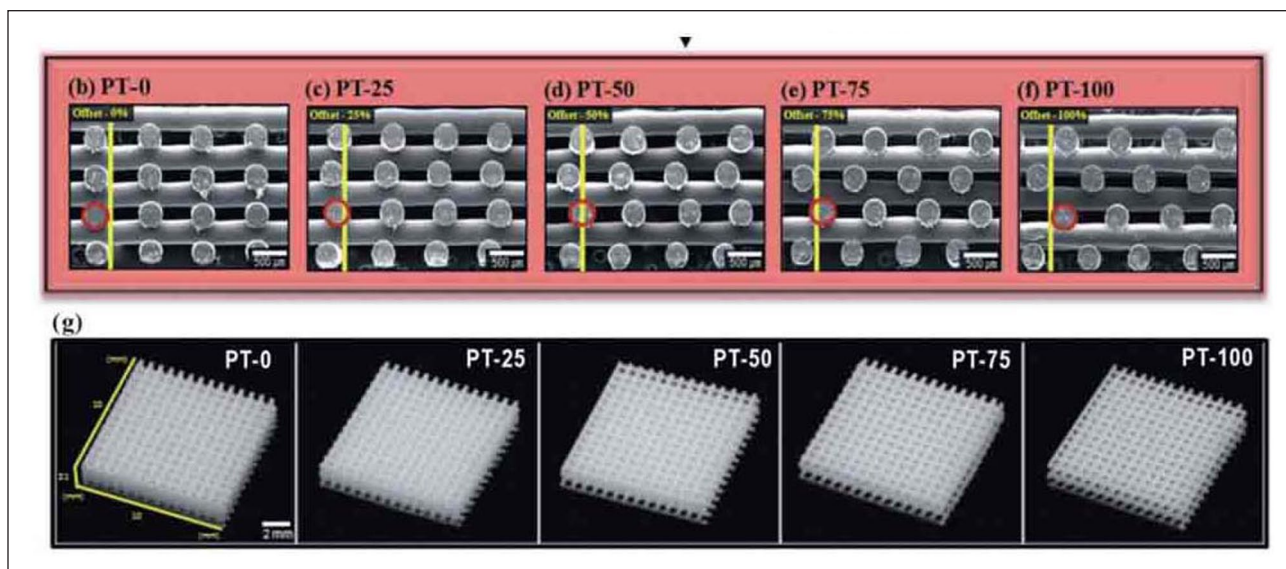
Figure 4. Schematic illustration of the design of different structured Polycaprolactone scaffold. (b–f) Cross-sectional scanning electron microscopy images of various scaffolds with various offset values. (g) Optical images of scaffolds.[22] Copyright ©2012 Royal Society of Chemistry (figure reused with permission).

proliferation numbers on the B, BO, C, and CO scaffolds as 235,000, 262,000, 222,000, and 28,700, respectively, demonstrating higher cell proliferation in scaffolds with an offset. Park et al.[9] reported that human osteosarcoma (MG 63) cells on PCL/HA/SP scaffolds had a higher cell proliferation rate compared to PCL and PCL/HA scaffolds. Additionally, researchers measured the total protein content to evaluate cell proliferation after 21 days. The total protein content in the scaffolds with compacted designs was remarkably higher compared to the scaffolds with the typical 0/90 pattern. These results could be attributed to an increased total surface area for cell adhesion in scaffolds with compacted designs.

The impact of different offset patterns on cell differentiation has also been evaluated previously. Yilgor et al.[13] measured alkaline phosphatase (ALP) activities, which are early osteoblastic differentiation markers, and the scaffolds with offset designs had a high expression of ALP. Cho et al.[11] demonstrated that the value of the ALP concentration of Offset 2 was superior to that of Offset 1 at day 7, owing to the preferable pore size. Yeo et al.[22] reported that scaffolds with 100% and 50% offset values showed greater ALP activities compared with any other offset scaffold. They also exhibited increased calcium mineralization in comparison with the scaffold without offset patterns (PT-0) at day 14. Moreover, when cultured in an osteogenic medium for more than 14 days, studies showed that more compacted structure (0/45 and 0/ 90 NP) promoted ALP expression. In addition to higher ALP activities, Col1a1, the osteoclasts marker, was at its peak after 7–14 days on the scaffolds with offset designs compared to the conventional scaffold design (0/90). Further, Bglap, a late

osteogenic marker, also up-regulated at day 14 or 21 in all the scaffolds with compacted architectures.[17]

Effect of the staggered structure on tissue engineering. Staggered structures also affect expression levels of angiogenesis-related factors and bone regeneration. Abbasi et al.[19] designed five different scaffolds coated with PCL and calcium phosphate (CaP) using MEW, including scaffolds with pore sizes of 250 μm or 500 μm, offset.50.50 (scaffolds with pore size of 500 μm and 50% offset), and two gradient scaffolds. Subsequently, bone repair and vascularization were evaluated using a critical-size calvarial defect model. Immunohistochemistry staining showed the highest staining of vascular endothelial growth factor and a higher expression of CD105 in the offset.50.50 structures after 8 weeks. Newly formed bone growing into the scaffolds was observed via Micro-CT, which showed that new bone distribution was more on the periphery of the offset.50.50 structures rather than the central region.

Discussion

Researchers have investigated the relationship between scaffolds with staggered patterns and their mechanical properties, water-uptake ability, cell activity, and bone regeneration.[10–23] Our analysis suggests that the incorporation of staggered designs can help in tuning their mechanical properties and water-uptake ability of scaffolds. Most studies have demonstrated that staggered designs have lower moduli compared to the non-staggered designs. This is because of the juxtaposition of continuous fiber along the z-axis direction in different non-staggered

Table 2. Mechanical and biological properties of the analyzed scaffolds.

Scaffolds Design	Mechanical properties	Biological properties	Bone regeneration or ALP
PCL PCL/HA PCL/HA/SP	The compression moduli of PCL and PCL/HA was significantly higher than the PCL/HA/SP scaffold.	MG 63 cells on PCL/HA/SP scaffolds had a higher cell adhesion and cell proliferation rate.	ALP expression of the PCL/HA/SP scaffolds was significantly enhanced compared to the PCL and PCL/HA scaffolds.
90°/500 mm/aligned 45°/500 mm/aligned 90°/1000 mm/aligned 45°/1000 mm/aligned 90°/1000 mm/offset 45°/1000 mm/offset	—	—	45°/500 mm/aligned scaffolds achieved the highest osteointegration score.
Conv 1, Conv 2, Offset 1, Offset 2, and dual pore	The compressive moduli of the Conv 1 and Conv 2 were higher than those of the Offset 1 and Offset 2 scaffolds.	Cell growth value of Offset 2 scaffolds were superior to those of the Conv 2 and Offset 1 scaffolds at 7 days.	The value of the ALP concentration of Offset 2 was superior to that of Offset 1 at day 7.
GEHA20 GEHA20-ZZ or GEHA20-ZZS GEHA20-45 or GEHA20-45S	—	The GEHA20-ZZS and GEHA20-45S scaffolds showed the highest proliferation.	The GEHA20-ZZS and GEHA20-45S had the highest ALP activity.
Basic(B), basic-offset (BO), crossed(C) and crossed-offset (CO)	The storage modulus of BO and CO are higher.	A higher cell numbers and cell adhesion on BO and CO .	Higher ALP activities on BO and CO.
The oriented scaffolds (basic, basic-offset) random scaffolds	—	Cell proliferation on random scaffolds was significantly higher.	—
Scaffolds with 45° and 90° layer rotation	The 0/45scaffold was stiffer than the 0/90 0scaffold.	—	—
0/90/0/90S 0/45/0/90NP	—	Compact scaffold architectures (0/90NP, 0/45, 0/90) positively influenced the seeding efficiency.	Scaffolds with 0/45 and 0/90 NP promoted ALP expression.
Grad 1, Grad 2, Homog 1, Homog 2	Young's modulus of the scaffolds Grad 1 and Grad 2 are in between Homog 1 and Homog 2.	The Grad 1 and Grad 2 improved seeding efficiency from 35% to70% and have a more even distribution of cells.	—
Scaffolds with lattice, stagger, and triangle design	The compression strength of scaffolds with triangular scaffolds was highest.	No significant differences in cell adhesion and proliferation.	—
Scaffolds with pore sizes of 250 and 500 µm, Scaffolds with pore sizes of 500 µm with 50% fiber offset Scaffolds with different pore sizes: 750–500-250µm (grad.750top) and 250–500–750 µm (grad.250top)	—	—	New bone distribution was more on the periphery of the offset.500.50 structures rather than the central region.
G, GS	The scaffolds of G and GS meso-structures showed much softer Properties.	—	—
Scaffolds with the offset value (0%, 25%, 50%, 75%, and 100%)	The elastic modulus of PT-100 was 7.4% higher than that of PT-0.	Scaffolds with offset patterns exhibited higher efficiencies than no-offset scaffolds.	Scaffolds with 100% and 50% offset values showed greater ALP activities compared with any other offset scaffold.
Scaffolds with different pore sizes of 250, 500, or 750 µm scaffolds with 30% or 50% offset gradient scaffold with pore sizes of 250–500–750 µm	—	—	Osteocalcin and osteopontin genes were upregulated in offset and gradient scaffold structures. Matrix mineralization was higher in the 50% offset scaffolds.

designs of the scaffold. As for biological properties, scaffolds with different offsets are beneficial for homogenous cell distribution, increased cell adhesion, and cell proliferation. They also promote cell differentiation compared to the no-offset structure. In particular, for cell differentiation, a more open geometry (no offset) delays differentiation in comparison with more irregular and denser internal architectures. On the one hand, scaffolds with different staggered designs have a complex inner geometry, thus increasing the number of anchorage points and contact time between the cells and scaffolds[18] along with the uptake ability in different staggered scaffold designs.[39] Sussman et al.[40] reported that a spiral-structured 3D matrix increased cell attachment due to an improved surface to volume ratio and a more complex structure. On the other hand, the flow rate, which is the speed of the cell suspension flows within the scaffolds, might be conditioned by the scaffold with different staggered designs. A low flow rate is beneficial to cell adhesion at the strand surface and connection sites, whereas cell deposition tended to take place at the bottom of the well when the flow rate was high. This result was consistent with that reported by Marín et al.[41] They identified the effect of the suspension flow rate on cell adhesion inside scaffolds using a computational model. The results indicated that static seeding had higher efficiency than dynamic perfusion. More importantly, scaffolds with different offsets offered more anchoring sites for cell extensions and created different angles, affecting the biological aspects in living cells through mechano-transduction.[39]

However, other scientific studies provided conflicting results. Several studies have demonstrated that scaffolds with offset structures have no impact on cell distribution, proliferation, and differentiation. Sun et al.[15] reported difficulties in observing any apparent differences between the 0/45 and 0/90 patterns in cell distribution and proliferation. Lee et al.[20] used MC3T3-E1 cells to evaluate the cell response. After seeding on the three different scaffolds for 7 days, the optical density (OD) value was measured using the CCK-8 kit to assess cell adhesion and proliferation. Although a continuous increase in OD levels was observed in every scaffold, no significant difference was observed. Cho et al.[11] demonstrated that there was no difference in the value of the ALP concentration of Offset 2 and Offset 1 scaffolds.

As for the methods to evaluate the properties of scaffolds, FEA may be a more convenient way to assess the physical properties and compare the stress and strain that occur when cells seeded on scaffolds with different internal architectures are subjected to a mechanical load[24] apart from the actual compression test. Egan et al.[42] used FEA to quantify the relationship between elastic modulus, shear modulus, permeability, and porosity for each topology. In addition, the FEA predictions and the actual compression moduli of the fabricated scaffolds exhibited similar

trends.[11] However, linear FEA presents some disadvantages when used to investigate scaffold properties. The nonlinear stress-strain behavior under scaffold compression cannot be simulated using linear FEA.[21] Liu et al.[21] used FEA and compression tests to access the mechanical properties of scaffolds with meso-structures. Based on the results, a relative error of 16.5% between the prediction and experiment was observed for the GS15 scaffolds (gradient and staggered scaffolds with strand orientation of 15) owing to the use of linear FEA.

In conclusion, the modification of the scaffold microstructure can regulate its physical and biological properties. From the standpoint of scaffold architecture, it mainly affects two aspects: surface area and flow rate. A higher surface area promotes cell activity, and flow rate can influence nutritional exchange, which is a vital pathway for cell growth and tissue regeneration.[43] This explains why a high permeability promotes cellular differentiation.[44]

Future studies

The above studies suggest that scaffolds with a staggered structure can potentially be extensively applied in tissue engineering. However, most studies are at the in vitro cell-culture experimental stage. To apply staggered scaffolds in clinical therapy, in vivo studies, especially pertaining to staggered structures promoting vessel formation and bone information, are required. Further, immune response, especially macrophage polarization, serves an important regulatory role in the prognosis of surgery or scaffold implantation.[45] Guo et al.[46] designed three types of scaffolds with varying substrate moduli (5–266 MPa). Scaffolds with a substrate modulus of 24 MPa enhanced the regenerative responses. It was associated with activating Wnt/β-catenin signaling and promoting the phenotypic transition of macrophages to the M2 anti-inflammatory macrophage. Therefore, the stimulation of recruiting/polarizing immune cells via the staggered structure needs to be further studied.

With improved software and computing hardware performance, other computational methods can be used to evaluate the mechanical and cellular responses. A mechanobiological model can evaluate the designs in a pre-manufactured design phase and predict tissue growth[47] prior to in vivo and in vitro experiments. Recently, artificial intelligence (AI) has been applied to tissue engineering, and AI can provide useful information for designers in the field of regenerative medicine.[48] Qiu et al.[49] reviewed related research on AI-associated privileged scaffolds. They emphasized on many aspects of research, including updates to the knowledge on privileged scaffolds, means of identifying privileged scaffolds, and new designs to replace conventional strategies. In the future, AI may be used to perform tests on scaffold properties and could help to discover highly optimized models,

reduce the workload, achieve better discoveries, and deepen our understanding of scaffolds.

Conclusion

This review summarized the current state of research on scaffolds with staggered patterns for tissue engineering applications. This type of scaffold can control its mechanical properties and affect cell adhesion, colonization, differentiation, and bone regeneration. However, only 15 related studies were truly consistent with the topic of this literature review, whose results were validated primarily via in vitro studies. Additionally, no study had the exact same model and set-up, leading to possibly inconclusive cross-comparisons. Therefore, the performance of scaffolds with offset patterns or staggered structures in vivo should be further studied in the near future. More studies are also required to clarify the effect of the scaffold microstructure on the mechanical properties and cell response. AI may aid the development of new designs for tissue engineering applications. AI can also be used to perform tests on scaffold properties and conduct in vivo and in vitro experiments. This review provides a foundation for future research directions.

Author contributions

X.H. literature review, performed data analysis, and drafted the manuscript. Q.Z., N.Z., and J.W. assistance in searching the literature. Y.X. revised the manuscript. Z.X. and Q.S. is the corresponding author who conceptualized the study, and edited the manuscript. All co-authors have seen the manuscript.

Declaration of conflicting interests

The author(s) declared no potential conflicts of interest with respect to the research, authorship, and/or publication of this article.

Funding

Guarantor

Z.X. and S.Q.

ORCID iDs

Xiaoli He https://orcid.org/0000-0002-5323-1174

Zhe Xing https://orcid.org/0000-0002-7419-2012

References

1. Panetta NJ, Gupta DM and Longaker MT. Bone regeneration and repair. *Curr Stem Cell Res Ther* 2010; 5: 122–128.
2. Li JJ, Ebied M, Xu J and Zreiqat H. Current approaches to bone tissue engineering: the interface between biology and engineering. *Adv Healthc Mater* 2018; 7: e1701061.
3. Fernandez de Grado G, Keller L, Idoux-Gillet Y, et al. Bone substitutes: a review of their characteristics, clinical use, and perspectives for large bone defects management. *J Tissue Eng* 2018; 9: 2041731418776819.
4. Dimitriou R, Jones E, McGonagle D and Giannoudis PV. Bone regeneration: current concepts and future directions. *BMC Med* 2011; 9: 66.
5. Chia HN and Wu BM. Recent advances in 3D printing of biomaterials. *J Biol Eng* 2015; 9: 4.
6. Murphy CM, Haugh MG and O'Brien FJ. The effect of mean pore size on cell attachment, proliferation and migration in collagen-glycosaminoglycan scaffolds for bone tissue engineering. *Biomaterials* 2010; 31: 461–466.
7. Woodfield TB, Malda J, de Wijn J, Péters F, Riesle J and van Blitterswijk CA. Design of porous scaffolds for cartilage tissue engineering using a three-dimensional fiber-deposition technique. *Biomaterials* 2004; 25: 4149–4161.
8. Nelson CM and Bissell MJ. Of extracellular matrix, scaffolds, and signaling: tissue architecture regulates development, homeostasis, and cancer. *Annu Rev Cell Dev Biol* 2006; 22: 287–309.
9. Park SA, Lee SH and Kim WD. Fabrication of porous polycaprolactone/hydroxyapatite (PCL/HA) blend scaffolds using a 3D plotting system for bone tissue engineering. *Bioprocess Biosyst Eng* 2011; 34: 505–513.
10. Hallman M, Driscoll JA, Lubbe R, et al. Influence of geometry and architecture on the in vivo success of 3D-printed scaffolds for spinal fusion. *Tissue Eng Part A* 2021; 27: 26–36.
11. Cho YS, Gwak SJ and Cho YS. Fabrication of polycaprolactone/Nano hydroxyapatite (PCL/nHA) 3D scaffold with enhanced in vitro cell response via design for Additive Manufacturing (DfAM). *Polymers* 2021; 13:1394. DOI: 10.3390/polym13091394
12. Kim JW, Han YS, Lee HM, Kim JK and Kim YJ. Effect of morphological characteristics and biomineralization of 3D-Printed gelatin/hyaluronic acid/hydroxyapatite composite scaffolds on bone tissue regeneration. *Int J Mol Sci* 2021; 22: 6794.
13. Yilgor P, Sousa RA, Reis RL, Hasirci N and Hasirci V. 3D plotted PCL scaffolds for stem cell based bone tissue engineering. *Macromol Symp* 2008; 269: 92–99.
14. Yilgor P, Sousa RA, Reis RL, Hasirci N and Hasirci V. Effect of scaffold architecture and BMP-2/BMP-7 delivery on in vitro bone regeneration. *J Mater Sci Mater Med* 2010; 21: 2999–3008.
15. Sun Y, Finne-Wistrand A, Albertsson AC, et al. Degradable amorphous scaffolds with enhanced mechanical properties and homogeneous cell distribution produced by a three-dimensional fiber deposition method. *Int J Biomed Mater Res* 2012; 100A: 2739–2749.
16. Kim YB and Kim GH. PCL/alginate composite scaffolds for hard tissue engineering: fabrication, characterization, and cellular activities. *ACS Comb Sci* 2015; 17: 87–99.

17. Declercq HA, Desmet T, Berneel EE, Dubruel P and Cornelissen MJ. Synergistic effect of surface modification and scaffold design of bioplotted 3-D poly-ε-caprolactone scaffolds in osteogenic tissue engineering. *Acta Biomater* 2013; 9: 7699–7708.

18. Sobral JM, Caridade SG, Sousa RA, Mano JF and Reis RL. Three-dimensional plotted scaffolds with controlled pore size gradients: Effect of scaffold geometry on mechanical performance and cell seeding efficiency. *Acta Biomater* 2011; 7: 1009–1018.

19. Abbasi N, Lee RSB, Ivanovski S, Love RM and Hamlet S. In vivo bone regeneration assessment of offset and gradient melt electrowritten (MEW) PCL scaffolds. *Biomater Res* 2020; 24: 17.

20. Lee J-S, Cha HD, Shim J-H, Jung JW, Kim JY and Cho DW. Effect of pore architecture and stacking direction on mechanical properties of solid freeform fabrication-based scaffold for bone tissue engineering. *Open J Biomed Mater Res* 2012; 100A: 1846–1853.

21. Liu H, Ahlinder A, Yassin MA, Finne-Wistrand A and Gasser TC. Computational and experimental characterization of 3D-printed PCL structures toward the design of soft biological tissue scaffolds. *Mater Des* 2020; 188: 108488.

22. Yeo M, Simon CG and Kim G. Effects of offset values of solid freeform fabricated PCL–β-TCP scaffolds on mechanical properties and cellular activities in bone tissue regeneration. *J Mater Chem* 2012; 22: 21636–21646.

23. Abbasi N, Ivanovski S, Gulati K, Love RM and Hamlet S. Role of offset and gradient architectures of 3-D melt electrowritten scaffold on differentiation and mineralization of osteoblasts. *Biomater Res* 2020; 24: 2.

24. Bose S, Vahabzadeh S and Bandyopadhyay A. Bone tissue engineering using 3D printing. *Mater Today* 2013; 16: 496–504.

25. Xie C, Gao Q, Wang P, et al. Structure-induced cell growth by 3D printing of heterogeneous scaffolds with ultrafine fibers. *Mater Des* 2019; 181: 108092.

26. Mieszczanek P, Robinson TM, Dalton PD and Hutmacher DW. Convergence of machine vision and melt electrowriting. *Adv Mater* 2021; 33: e2100519.

27. Kade JC and Dalton PD. Polymers for melt electrowriting. *Adv Healthc Mater* 2021; 10: e2001232.

28. Brun PT, Audoly B, Ribe NM, Eaves TS and Lister JR. Liquid Ropes: A geometrical model for thin viscous jet instabilities. *Phys Rev Lett* 2015; 114: 174501.

29. Ribe NM, Lister JR and Chiu-Webster S. Stability of a dragged viscous thread: onset of "stitching" in a fluid-mechanical "sewing machine. *Phys Fluids* 2006; 18: 124105.

30. Hochleitner G, Chen F, Blum C, Dalton PD, Amsden B and Groll J. Melt electrowriting below the critical translation speed to fabricate crimped elastomer scaffolds with non-linear extension behaviour mimicking that of ligaments and tendons. *Acta Biomater* 2018; 72: 110–120.

31. Bar-On B and Wagner HD. Elastic modulus of hard tissues. *J Biomech* 2012; 45: 672–678.

32. Ji B and Gao H. Mechanical Principles of Biological Nanocomposites. *Annu Rev Mater Res* 2010; 40: 77–100.

33. Wu L and Ding J. In vitro degradation of three-dimensional porous poly(d,l-lactide-co-glycolide) scaffolds for tissue engineering. *Biomaterials* 2004; 25: 5821–5830.

34. Lohfeld S, Cahill S, Doyle H and McHugh PE. Improving the finite element model accuracy of tissue engineering scaffolds produced by selective laser sintering. *J Mater Sci Mater Med* 2015; 26: 5376.

35. Moroni L, de Wijn JR and van Blitterswijk CA. 3D fiber-deposited scaffolds for tissue engineering: influence of pores geometry and architecture on dynamic mechanical properties. *Biomaterials* 2006; 27: 974–985.

36. Hutmacher DW, Schantz T, Zein I, Ng KW, Teoh SH and Tan KC. Mechanical properties and cell cultural response of polycaprolactone scaffolds designed and fabricated via fused deposition modeling. *J Biomed Mater Res* 2001; 55: 203–216.

37. Goldstein SA. The mechanical properties of trabecular bone: dependence on anatomic location and function. *J Biomech* 1987; 20: 1055–1061.

38. Dowling DP, Miller IS, Ardhaoui M and Gallagher WM. Effect of surface wettability and topography on the adhesion of osteosarcoma cells on plasma-modified polystyrene. *J Biomater Appl* 2011; 26: 327–347.

39. Abbasi N, Abdal-hay A, Hamlet S, Graham E and Ivanovski S. Effects of gradient and offset architectures on the mechanical and biological properties of 3-D Melt electrowritten (MEW) scaffolds. *ACS Biomater Sci Eng* 2019; 5: 3448–3461.

40. Sussman M, Bohak Z and Kadouri A. *Fibrous matrix for in vitro cell cultivation*. United States United STATES Patent US19920869078, 1993.

41. Campos Marín A, Brunelli M and Lacroix D. Flow perfusion rate modulates cell deposition onto scaffold substrate during cell seeding. *Biomech Model Mechanobiol* 2018; 17: 675–687.

42. Egan PF, Gonella VC, Engensperger M, Ferguson SJ and Shea K. Computationally designed lattices with tuned properties for tissue engineering using 3D printing. *PLoS One* 2017; 12: e0182902.

43. Wintermantel E, Mayer J, Blum J, Eckert KL, Lüscher P and Mathey M. Tissue engineering scaffolds using superstructures. *Biomaterials* 1996; 17: 83–91.

44. Kemppainen JM and Hollister SJ. Differential effects of designed scaffold permeability on chondrogenesis by chondrocytes and bone marrow stromal cells. *Biomaterials* 2010; 31: 279–287.

45. Barros MH, Hauck F, Dreyer JH, Kempkes B and Niedobitek G. Macrophage polarisation: an immunohistochemical approach for identifying M1 and M2 macrophages. *PLoS One* 2013; 8: e80908.

46. Guo R, Merkel AR, Sterling JA, Davidson JM and Guelcher SA. Substrate modulus of 3D-printed scaffolds regulates the regenerative response in subcutaneous implants through the macrophage phenotype and Wnt signaling. *Biomaterials* 2015; 73: 85–95.

47. Egan PF. Integrated design approaches for 3D printed tissue scaffolds: review and outlook. *Materials* 2019; 12: 12.

48. Bermejillo Barrera MD, Franco-Martínez F and Díaz Lantada A. Artificial intelligence aided design of tissue engineering scaffolds employing virtual tomography and 3D convolutional neural networks. *Materials* 2021; 14: 14.

49. Qiu HY, Clausen RP, He Y and Zhu HL. Artificial intelligence and cheminformatics-guided modern privileged scaffold research. *Curr Top Med Chem* 2021; 21: 2593–2608.